



Contents lists available at ScienceDirect

Acta Histochemica

journal homepage: [www.elsevier.com/locate/acthis](http://www.elsevier.com/locate/acthis)

## Nanomicelle curcumin-induced DNA fragmentation in testicular tissue; Correlation between mitochondria dependent apoptosis and failed PCNA-related hemostasis

Sana Moshari<sup>a</sup>, Vahid Nejati<sup>a,\*</sup>, Gholamreza Najafi<sup>b</sup>, Mazdak razi<sup>b</sup>

<sup>a</sup> Department of Biology, Faculty of Basic Science, Urmia University, Urmia, Iran

<sup>b</sup> Department of Basic Science, Faculty of Veterinary Medicine, P.O. BOX: 1177, Urmia University, Urmia, Iran

### ARTICLE INFO

#### Keywords:

Nanomicelle curcumin  
Spermatogenesis  
Apoptosis  
Testosterone

### ABSTRACT

Current study was done to assess possible anti-proliferative effect of nanomicelle curcumin (NMCM) against germ cells in testicular tissue. For this purpose, 24 mature male Wistar rats were divided into control and test groups. The animals in test groups received 7.5 mg/kg, 15 mg/kg and 30 mg/kg of NMC (NO = 6 rats in each group). Following 48 days, the expression of Bcl-2, Bax, caspase-3, P53 and proliferating cell nuclear antigen (PCNA) were evaluated by using reverse transcription-PCR and immunohistochemistry. Histological changes, tubular differentiation index (TDI), tissue cellularity and serum level of testosterone were analyzed. Finally, the DNA laddering test was used to assess the DNA fragmentation as hallmark for apoptosis. The NMCM significantly ( $P < 0.05$ ) diminished the Bcl-2, p53 and PCNA and enhanced the Bax and caspase-3 mRNA levels. The NMCM significantly ( $P < 0.05$ ) elevated the percentage of Bax and caspase-3-positive tubules and remarkably reduced the percentage of tubules with positive reaction for Bcl-2, p53 and PCNA. The NCMN-received animals exhibited remarkable ( $P < 0.05$ ) reduction in cell population, TDI ratio and serum level of testosterone. Severe DNA fragmentation was observed in 30 mg/kg NMCM-received group. In conclusion, the NMCM by reducing the testicular endocrine status, down-regulating Bcl-2 expression and by enhancing the Bax and caspase-3 expression initiates the intrinsic apoptosis pathway. On the other hand, inhibited expression of p53 and PCNA (at dose level of 30 mg/kg) suppresses the p53 and PCNA-related hemostasis/preservative reactions. All these alterations adversely affect the spermatogenesis.

### 1. Introduction

Curcumin (CMN), primary ingredient of Tumeric (*Curcuma Longa*), has been known as the main part of Indians condiment (Choudhary and Sekhon, 2012). Multiple therapeutic properties of the CMN are well established in several investigations. Accordingly, anti-inflammatory, antioxidant and anticancer effects have been reported for CMN-related remedial traits (Malani and Ichikawa, 2007). Among several characteristics of CMN, its anti-proliferative impact on carcinogenic cells has attracted a lot of attentions. Earlier study by Mehta et al. (1997) showed that, the CMN results in cell cycle arrest at G2/S phase in breast tumor cell lines in vitro (Mehta et al., 1997). More recent studies have shown the CMN-induced anti-proliferative/anti-growth impacts at other stages as G2/M in breast tumor cells (Kumaravel et al., 2012) as well as G0/G1 stages in pancreatic stellate cells (Gundewar et al., 2015). More

characteristics including; inhibiting ornithine decarboxylase activity (Mehta et al., 1997), downregulating p21<sup>WAF1/Cip1</sup> expression (Gundewar et al., 2015) and diminishing of cyclin D1, cyclin E, cyclin A, cyclin-dependent kinase 2 (CDK2) and CDK4 expression as well as inducing cell cycle inhibitor p21 and p27 expression are reported, representing the anti-proliferative effect of CMN (Kumaravel et al., 2012; Zhou et al., 2011). Aside the anti-proliferative impacts, the CMN has been known as pro-apoptotic agent in various studies. Accordingly, the CMN by activating the JNK/ERK (Yang et al., 2012), p38 mitogen-activated protein kinase (Hu et al., 2005), miR-192-5p/215 induction and the p53-miR-192-5p/215-XIAP pathways (Ye et al., 2015) stimulates or initiates apoptosis in different cell lines. Moreover, last researches have shown the involvement of CMN in p53-dependent apoptosis pathways (Keshavarz et al., 2016; Li et al., 2015). In another study, Cao et al. (2006), have illustrated the impressive effect of CMN

**Abbreviation:** CMN, curcumin; NMCM, nanomicelle curcumin; PCNA, proliferating cell nuclear antigen; TDI, tubular differentiation index; CDK 2, cyclin dependent kinase 2; CAD, caspase activated DNase; RFC, replication factor C

\* Corresponding author.

E-mail address: [V.nejati@urmia.ac.ir](mailto:V.nejati@urmia.ac.ir) (V. Nejati).

<http://dx.doi.org/10.1016/j.acthis.2017.03.007>

Received 8 February 2017; Received in revised form 25 March 2017; Accepted 25 March 2017  
0065-1281/ © 2017 Published by Elsevier GmbH.

on mitochondrial and nuclear DNA integrity by illustrating impressive DNA damage in human hepatoma G2 cells (Cao et al., 2006).

In male reproductive system, mature spermatozoa are produced during spermatogenesis process in seminiferous tubules (Shaha et al., 2010). Through physiologic spermatogenesis, the spermatogonial stem cells proliferate through mitosis and meiosis divisions and then differentiate in order to constantly generate spermatozoa (Kolasa et al., 2012). Minding high incidence of mitosis and meiosis during spermatogenesis, the anti-proliferative agents are able to disrupt cell division similar to carcinogenic condition. For instance, it has been shown that, the anti-proliferative agents as well as chemotherapeutic and/or pro-apoptotic chemicals adversely affect spermatogenesis process by breaking the mitosis and meiosis processes (Meistrich, 2013; Ragheb and Sabaneh, 2010; Uygur et al., 2014).

Several genes (more than 500 genes) such as p53, E2f1, p21, cyclins and cyclin dependent kinases are known as checkpoint machinery system during cell cycle. These genes initiate apoptosis at different phases following mutation and/or DNA damage (Ortega et al., 2003; Rotgers et al., 2015; Western et al., 2008). Therefore any pro-apoptotic stimuli agents impressively initiate cell elimination, resulting in spermatogenesis arrest. Indeed, the DNA damage is considered as main initiator of apoptosis, which alters tumor suppressor P53 and Proliferating cell nuclear antigen (PCNA) genes expression among several same-targeting genes (Lukas et al., 2011; Xu et al., 2011). It should note that, the p53 controls the G1/S and G2/M cell cycle borders for probable DNA damage. In fact, the DNA damage up-regulates the p53 expression leading to apoptosis and/or possible DNA repairment (Lu et al., 2010; Lukas et al., 2011). On the other hand, the proliferating cell nuclear antigen (PCNA) is known as a key factor involving in many essential cellular processes, including; DNA replication, DNA repair pathway, DNA damage avoidance and cell cycle control (Stoimenov and Helleday, 2009; Xu et al., 2011). During the p53-dependent apoptotic pathway, the p53 binds to Bcl-xl, induces Puma expression and triggers Bax and Bak oligomerization. Moreover it has been shown that, the P53 inhibits the anti-apoptotic effects of Bcl-2 and Bcl-xl (Amaral et al., 2010; Newshean and Yang, 2012; Tasdemir et al., 2008). In continue, caspases (especially the caspase-3) interact as finishers of apoptosis pathway (McIlwain et al., 2013).

The nanomicelles are known as biologically safe, non-genotoxic, non-cytotoxic agents. Thus, the nanosized micelles are widely used to enhance the pharmaceutical impact of several drugs (Trivedi and Kompella, 2010; Vadlapudi and Mitra, 2013; Yokoyama, 2014). Using these advantages, lastly the nanomicelle curcumin (NMCM) has been produced to promote the effectiveness and bioavailability of CMN. Given that, the CMN exerts anti-proliferative impact, here in present study we aimed to investigate possible anti-proliferative/pro-apoptotic effects of NMCM (more biologically stable form of CMN) against spermatogenesis. For this purpose, tubular repopulation and differentiation indices were analyzed as confirmed markers for cellular proliferation during spermatogenesis. Moreover, the hallmarks for apoptosis including; the possible changes in expression of p53, PCNA, Bcl-2, Bax and caspase-3 genes/proteins as well as the DNA fragmentation were investigated. Finally, we assessed the serum level of testosterone as clinical marker, reflecting the testicular spermatogenesis and endocrine potential.

## 2. Methods and materials

### 2.1. Chemicals and materials

The NMCM (10–100 nm) was obtained from Minoos Pharmaceutical Co., (Tehran, Iran). The primary antibodies for P53, Bcl-2, BAX and Caspase-3 proteins were purchased from life-Teb-Gen Co., (Tehran, Iran). Moreover, the primary antibody for PCNA was assigned from Khatibzadeh Co., (Tehran, Iran).

### 2.2. Animals and grouping

Twenty four mature male *Wistar* rats weighing 200–220 gr were assigned from the animal house, faculty of basic science, Urmia University, Urmia, Iran. All the animals were housed in a standardized environment (at  $23 \pm 2$  °C and 12/12 day/night photoperiod). Food (pellet diet) and water were available *ad libitum*. This study was conducted according to the instruction of Urmia University ethical committee based on the Laboratory Animal Care Ethics. The Rats were equally divided into 4 groups (No: 6 in each group), including control and three experimental groups. The animals in control group received normal saline (0.5 ml) as solvent for NMCM. The experimental groups received defined doses of NMCM (7.5 mg/kg, 15 mg/kg and 30 mg/kg). The final concentration of solvent was not exceeded from 5% of the administered normal saline. All animals received the chemicals for a 48 day period.

### 2.3. Tissue preparation and histological analyses

To perform histological analyses, the testes were dissected out under high magnification provided by Stereo Zoom Microscope (SZX16-olympus, Japan, 400×) and left testes fixed in Bouin's fixative (picric acid, acetic acid and formaldehyde) for 72 h. Thereafter, the right testes were stored in  $-80$  °C for further examination of biochemical and molecular parameters (see next). The fixed testicles routinely were passage through ascending degrees of ethanol (70%, 80%, 90%, 96% and 100%) and then embedded in paraffin. In continue, the paraffin blocks were cut (5 μm sections) by rotary microtome (Leitz Wetzlar, Germany). Iron-Wiegert staining, as special staining technique for detecting nuclei, was done in order to evaluate cell number per one seminiferous tubule. For this purpose, 20 tubules were considered in one cross section (120 tubules for each group) and the results were compared between groups. Moreover, the Leydig cells number per one mm<sup>2</sup> of interstitial connective tissue was assessed using the 100 square lens devise (Olympus, Germany) and the cell numbers were reported per one mm<sup>2</sup> of interstitial connective tissue and compared between groups.

### 2.4. Serum sampling and testosterone assessment

Following light anesthesia by 5% ketamine, 40 mg/kg, and 2% xylazine (Alfasan, Woerden, and The Netherlands), 5 mg/kg, the blood samples were collected directly from heart. Thereafter, the specimens were centrifuged at 3000g for 5 min. The serum samples were separated and considered for assessment of testosterone levels. Competitive enzymatic immunoassay kit (DRG, Germany) was used to evaluate serum testosterone. Moreover, the intra-assay and inter-assay coefficient variances were estimated as 3.9% and 6.8% for testosterone (for 10 times), respectively.

### 2.5. Immunohistochemical staining (IHC)

Following the tissue sections preparation, they were heated at 60 °C for 20 min in a hot air oven (Venticell, MMM, Einrichtungen, Germany). Then, the slides were de-paraffinized in xylene and rehydrated in descending concentrations of alcohol (90%, 80%, 70%, 50%) and transferred to the sodium citrate buffer (10 mM, PH = 7.2) for antigen retrieval process. Thereafter, 0.03% hydrogen peroxide solution was used to block endogenous peroxidase. The sections were washed with Phosphate-buffered saline (PBS) and subsequently incubated with primary antibody (Bcl-2, Bax, PCNA, P53 and Caspase-3), for 18 h in 4 °C. After washing the slides in washing buffer, they were transferred into the humidified chamber and incubated with Anti-polyvalent antibody and consequently with HRP (Horseradish peroxidase), each for 10 min. The slides were washed with PBS after each step. Afterwards the slides were incubated with a diaminobenzidine-

**Table 1**  
Antibodies, concentrations and details.

Name	Description	Species Reactivity	Concentration	Cat No:	Company
Anti-p53	Rabbit polyclonal to p53	Mouse, Rat, Human	1:600	Ab1431	Abcam, UK
Anti-Bcl2	Mouse polyclonal to Bcl-2	Human, Rat	1:500	AP10039	Gennova, Spain
Anti-Bax	Rabbit Polyclonal Antibody to BAX	Mouse	1:600	AB2915	Merck, Germany
Anti-Caspase-3	Rabbit Polyclonal Antibody to Caspase-3	Human, Mouse	1:200	PP 229 AA	Biocare, USA
Anti-PCNA	Rabbit Polyclonal Antibody to PCNA	Mouse, Rat, Sheep, Goat, Cow, Human, Monkey, Zebrafish, Common marmoset	1:500	Ab18197	Abcam, UK

**Table 2**  
Product sizes and sequences for used primers.

	Primer	Size
P53	5'- ATGGAGGAGTCACAGTCGGATA-3' 5'-GACTTCTGTAGATGCCATGG-3'	465 bp
Bcl-2	5' - CGCCCGCTGTGCACCGAGA-3' 5' - CACAATCTCCCCAGTTCACC-3'	260 bp
Caspase-3	5'-TACCCTGAAATGGGCTTGTGT-3' 5'-GTAAACACGAGTGAGGATGTG-3'	520 bp
BAX	5'AAGAAGCTGAGCGAGTGTCT-3' 5'CAAAGATGGTCACTGTCTGC-3'	260 bp
GAPDH	5'-GTTACCAGGGCTGCCTTCTC-3' 5'-GGGTTTCCCGTTGATGACC -3'	660 bp

substrate (DAB) chromogen for 10 min, followed by washing and counterstaining with hematoxylin for 10 s and were rinsed with distilled water and cover slipped. Positive IHC staining was observed as brown stains under a light microscope. The percentage of tubules with positive reaction for each antibody was estimated in each group and compared between groups. The antibodies, concentrations and details are presented in Table 1.

## 2.6. RNA extraction

The  $-80^{\circ}\text{C}$  stored testicular specimens were homogenized by homogenizer Precellys 24 (Bertin Technologies, Aix-en-Provence, France). The mRNA isolation was based on the standard TRIZOL

method (Chomczynski and Sacchi, 2006). The quality and purity of the extracted RNA were evaluated by NanoDrop-2000c spectrophotometer (Thermo Scientific, Washington, USA) at 260 nm and A260/280 nm (1.8–2.0), respectively.

## 2.7. cDNA synthesis and Reverse Transcription Polymerase Chain Reaction (RT-PCR)

For RT-PCR, the cDNA was synthesized in a 20  $\mu\text{l}$  reaction mixture containing 2  $\mu\text{g}$  RNA (3  $\mu\text{l}$ ), 1  $\mu\text{l}$  oligo (dT) primer, 4  $\mu\text{l}$  5  $\times$  reaction buffer, 1  $\mu\text{l}$  RNase inhibitor, 10 mM dNTP mix (2  $\mu\text{l}$ ) and M-MuLV Reverse Transcriptase (1  $\mu\text{l}$ ) according to the manufacturer's protocol (Fermentas, GmbH, Germany). The cycling protocol for 20  $\mu\text{l}$  reaction mix was 5 min at  $65^{\circ}\text{C}$ , followed by 60 min at  $42^{\circ}\text{C}$ , and 5 min at  $70^{\circ}\text{C}$  to terminate the reaction. The RT-PCR reaction was carried out in a total volume of 25  $\mu\text{l}$  containing PCR master mix (16  $\mu\text{l}$ ), FWD and REV specific primers (each 1  $\mu\text{l}$ ) and cDNA as a template (2  $\mu\text{l}$ ) and nuclease free water (5  $\mu\text{l}$ ). The PCR condition was run as follows: general denaturation at  $95^{\circ}\text{C}$  for 3 min, 1 cycle, followed by 35–40 cycles of  $95^{\circ}\text{C}$  for 20 s; annealing temperature [ $50^{\circ}\text{C}$  for caspase-3 (45 s),  $62^{\circ}\text{C}$  for Bcl-2 (1 min),  $59^{\circ}\text{C}$  for Bax (1 min),  $52^{\circ}\text{C}$  for p53 (1 min) and  $57^{\circ}\text{C}$  for GAPDH (1 min)]; elongation:  $72^{\circ}\text{C}$  for 1 min and  $72^{\circ}\text{C}$  for 5 min. Specific primers (Kermer et al., 1999; Li et al., 2007; Rogerio et al., 2006; Soleimani Asl et al., 2012) were designed and manufactured by Cinna-Gen (Cinna-Gen Co.Tehran, Iran). Nucleotide sequences and products size for primers used in RT-PCR are presented in Table 2. Final PCR products were analyzed on 1.8% agarose gel electrophoresis

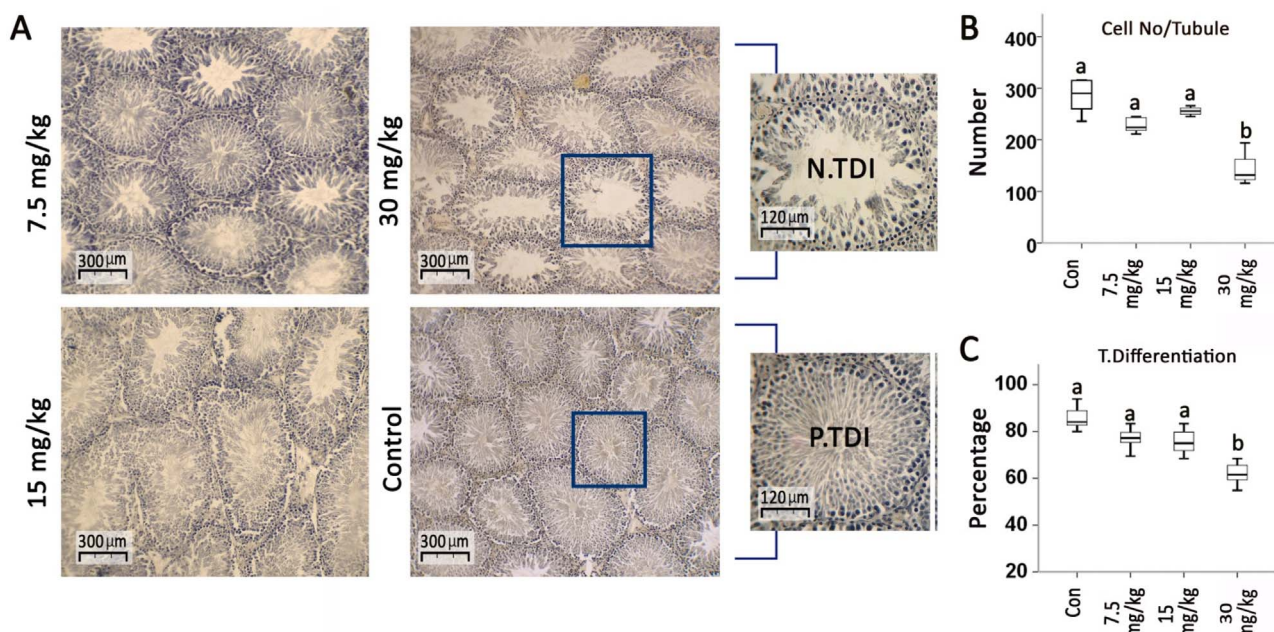


**Fig. 1.** (A) Cross section from testicles; **P.TDI**: positive tubular differentiation index and **N.TDI**: negative tubular differentiation index, (B) Mean cell number per one seminiferous tubule and (C) Percentage of seminiferous tubules with positive differentiation index in different groups. All data are presented in Mean  $\pm$  SD and <sup>a,b</sup> are representing significant differences ( $P < 0.05$ ) between marked groups.

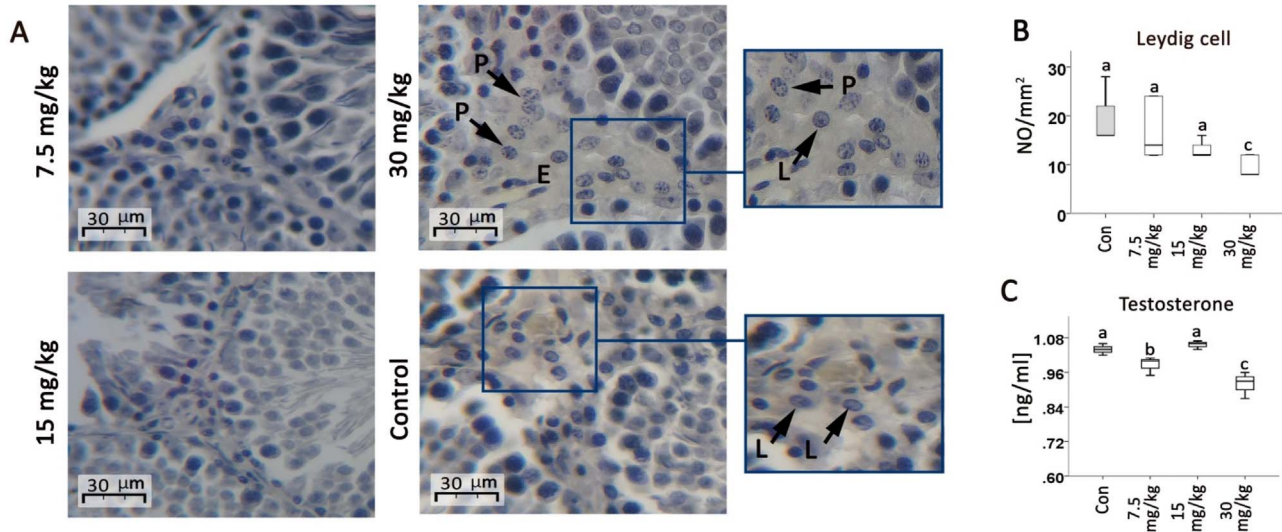


**Fig. 2.** (A) Cross section from testicular tissue; See decreased Leydig cells (L) and enhanced plasma cells (P) distribution in connective tissue of 30 mg/kg NMCM-received group, (B) Leydig cells number per one mm<sup>2</sup> of connective tissue and (C) serum level of testosterone in different groups. All data are presented in Mean  $\pm$  SD and <sup>a,b,c</sup> are representing significant differences ( $P < 0.05$ ) between marked groups.

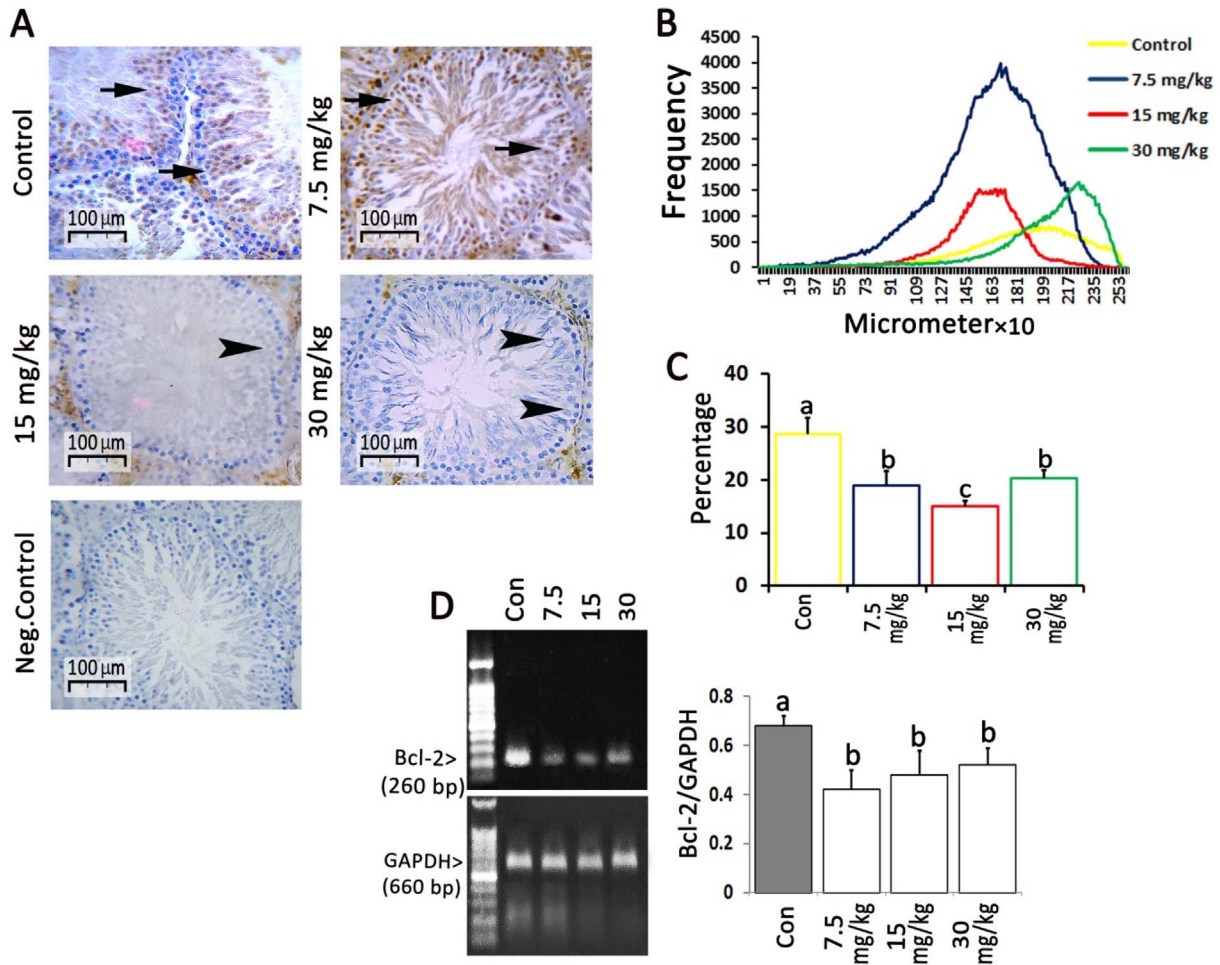


**Fig. 3.** (A) Immunohistochemical staining for Bcl-2; See intact seminiferous tubules with massive Bcl-2-positive cells (arrows) and those tubules with impaired spermatogenesis representing unstained cells (head arrows) in NMCM-received groups. **Neg. Control:** negative control, no primary antibody was use, (B) pixel based histogram analysis for Bcl-2 positive reaction in  $253 \times 10 \mu\text{m}$  of one cross section, (C) percentage of seminiferous tubules with positive reaction for Bcl-2 and (D) RT-PCR electrophoresis gel result. See relative semi-quantitative intensity (Bcl-2/GAPDH) for decreased Bcl-2 mRNA level in NMCM-received groups versus reaction control group. All data are presented in Mean  $\pm$  SD and <sup>a,b,c</sup> are representing significant differences ( $P < 0.05$ ) between marked groups.

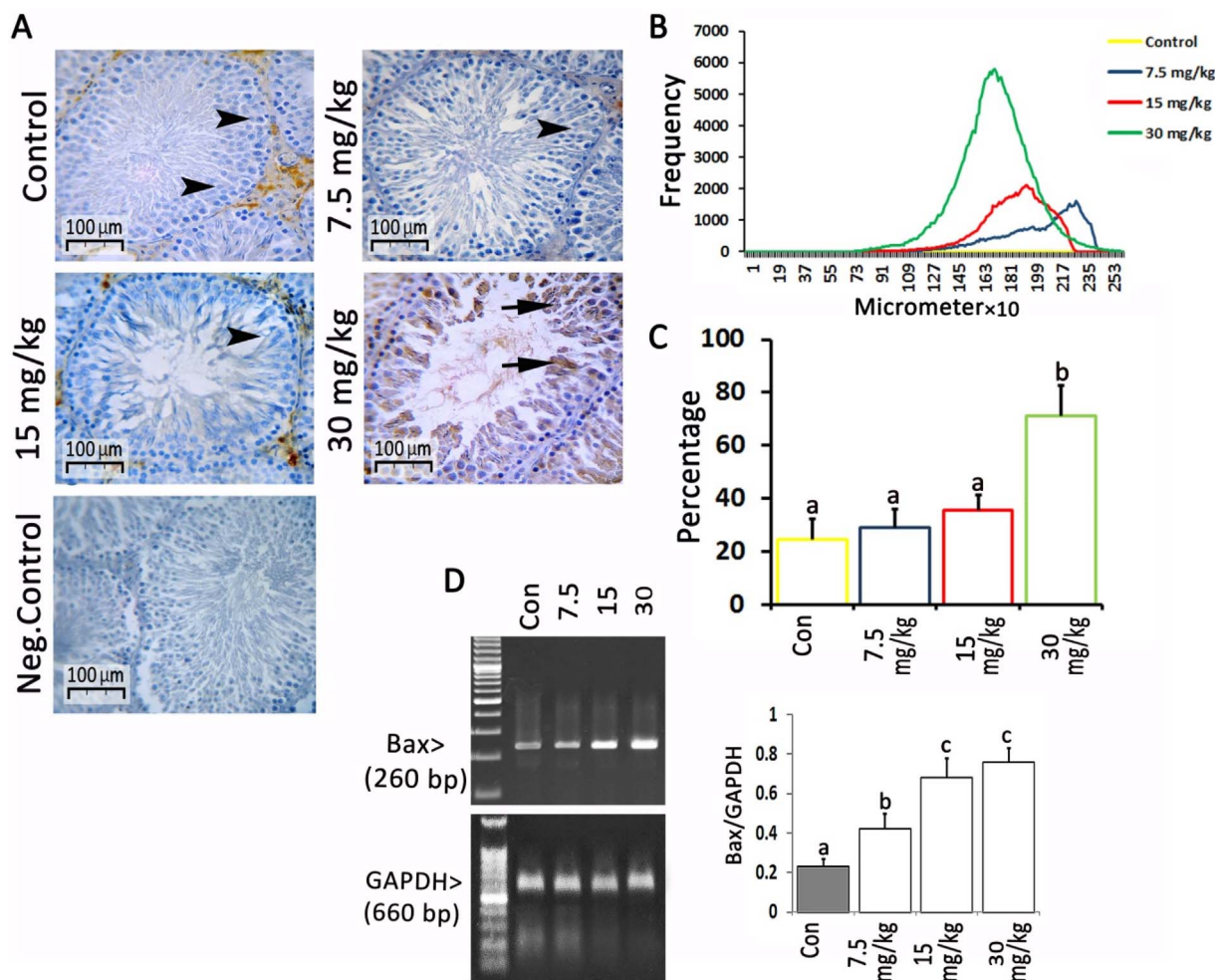


**Fig. 4.** (A) Immunohistochemical staining for Bax; See intact seminiferous tubules representing unstained cells (head arrows) and the tubule with impaired spermatogenesis which is presenting Bax-positive cells (arrows). **Neg. Control:** negative control, no primary antibody was used. (B) pixel based histogram analysis for Bax positive reaction in  $253 \times 10 \mu\text{m}$  of one cross section, (C) percentage of seminiferous tubules with positive reaction for Bax and (D) RT-PCR electrophoresis gel result. See relative semi-quantitative intensity (Bax/GAPDH) for increased Bax mRNA level in NMCM-received groups versus control group. All data are presented in Mean  $\pm$  SD and <sup>a,b,c</sup> are representing significant differences ( $P < 0.05$ ) between marked groups.

and densitometric analysis of the bands were done by using PCR Gel analyzing software (ATP, Tehran, Iran). The control was set at 100% and experimental samples were compared to the control.

## 2.8. DNA laddering test

In order to analyze the apoptosis-induced DNA fragmentation, the DNA laddering test was performed by using Cina Pure-DNA extraction kit (Sinaclon, Iran). For this purpose, 100  $\mu\text{l}$  from protease buffer was added to 35 mg of testicular tissues in a 1.5  $\mu\text{l}$  microcentrifuge tubes and then 5  $\mu\text{l}$  of protease was added into same tubes. Thereafter, the tubes were incubated in 55  $^{\circ}\text{C}$  for 2 h. Following incubation, the samples were completely homogenized and 100  $\mu\text{l}$  of samples were added into a new microcentrifuge tubes. After that, 400  $\mu\text{l}$  of lysis solution was added into the tubes. Extra cares were taken to avoid any clot and/or insoluble materials aggregation in tubes. Then, 300  $\mu\text{l}$  of precipitation solution (Isopropanol based) was added into the tubes and mixed by vortexing for 5 min. Following that, the tubes were centrifuged at 12000g for 10 min. The tubes then were decanted by gently inverting of tubes and placing the tubes on tissue paper for 2–3 s. Thereafter, 1 ml Wash Buffer (ethanol based) was added on pellets and mixed by 5 s vortexing and centrifuged at 12000g for 5 min (twice). The wash buffer was then poured off completely and the pellets were dried at 65  $^{\circ}\text{C}$  for 5 min. After that, the wall of tubes was washed by softly

pipetting for mixing of any residual pellet. Finally, unsolved materials were precipitated by centrifuging the tubes at 12000 g for 30 s and the DNA containing supernatant was picked up. The DNA content, quality and purity, were measured with a NanoDrop-1000 spectrophotometer (Thermo Scientific, Washington, USA). The eluted DNA was used directly. The DNA was quantified and a volume of elute corresponding to 2  $\mu\text{g}$  DNA (15–17  $\mu\text{l}$  of eluted DNA) was added to loading buffer (50% glycerol; 2 mm EDTA; 0.4% bromophenol blue), and the DNA solution was run on a 1% agarose gel for 70 min at 70-V constant voltage. PST1 also was loaded as a marker for identification of amount of DNA. Gels were stained with ethidium bromide and visualized by Gel Doc 2000 system (ATP, Tehran, Iran).

## 2.9. Statistical analyses and imaging

All results are presented as Mean  $\pm$  SD. Differences between quantitative histological and biochemical data were analyzed with one-way ANOVA, followed by Bonferroni test, using Graph Pad Prism, 4.00. A  $p < 0.05$  was considered as statistically significant. The photomicrographs were taken by SONY onboard camera (Zeiss, Cyber-Shot, Japan). Image pro-insight software (version 9.00) was used for evaluating the pixel based distribution of ER $\alpha$ , cyclin D1, Cdk4, p53 and p21 positive cell per  $253 \times 10 \mu\text{m}$ .

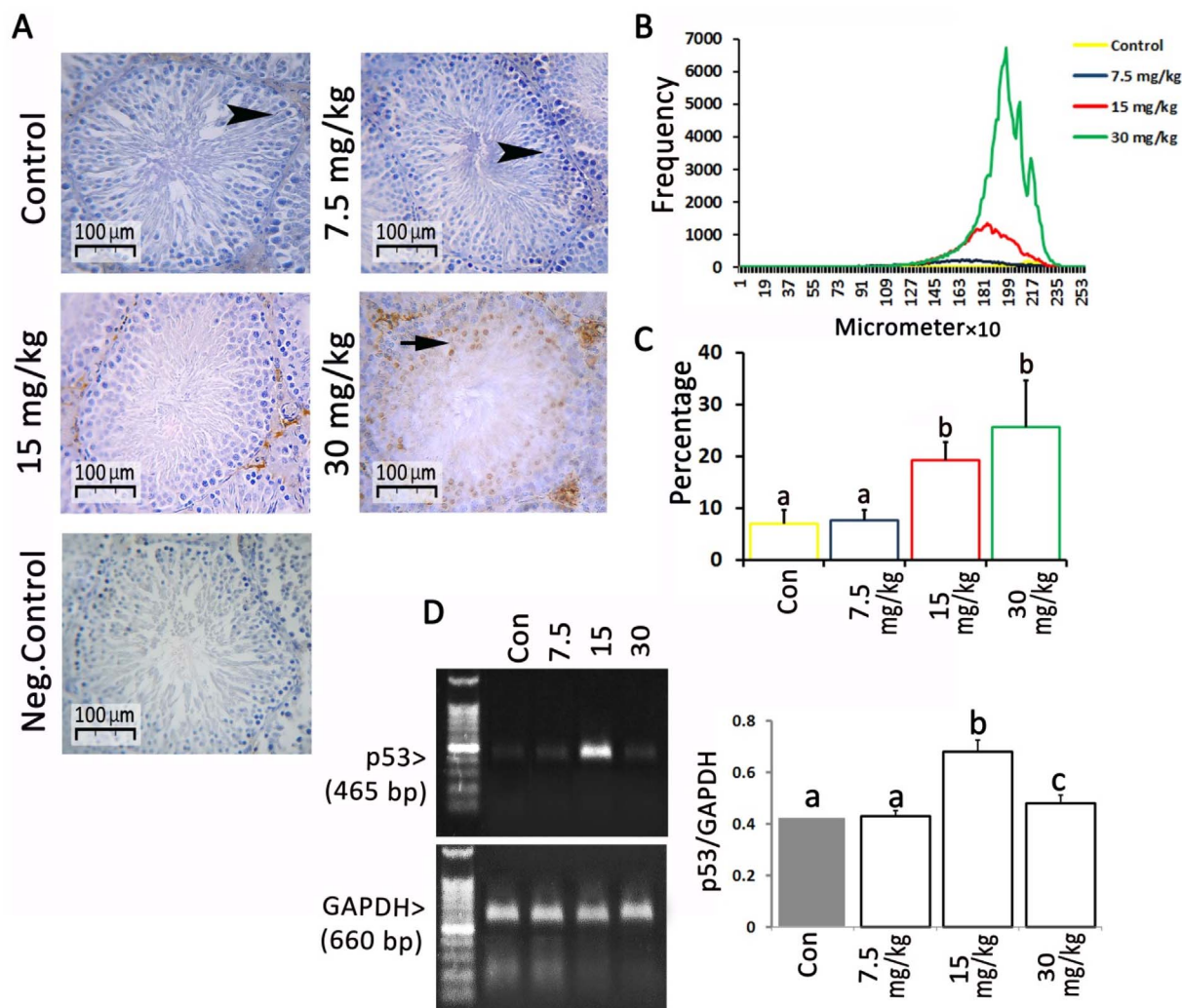


**Fig. 5.** (A) Immunohistochemical staining for p53; see intact seminiferous tubules representing unstained cells (head arrows) and the tubule with impaired spermatogenesis which is presenting p53-positive cells (arrows). **Neg. Control:** negative control, no primary antibody was use, (B) pixel based histogram analysis for p53 positive reaction in  $253 \times 10 \mu\text{m}$  of one cross section, (C) percentage of seminiferous tubules with positive reaction for p53 and (D) RT-PCR electrophoresis gel result. See relative semi-quantitative intensity (p53/GAPDH) for increased p53 mRNA level in NMCM-received groups versus control group. All data are presented in Mean  $\pm$  SD and <sup>a,b,c</sup> are representing significant differences ( $P < 0.05$ ) between marked groups.

### 3. Results

#### 3.1. Histological and serum analysis

The adverse impact of NMCM on cellular proliferation was analyzed by evaluating cellularity (cells number per one seminiferous tubule) and by assessing the differentiation index. Accordingly, the animals in NMCM-received groups (especially those in 30 mg/kg-received group) exhibited diminished tubular differentiation index as well as decreased ( $P < 0.05$ ) cell number per one tubule versus control group (Fig. 1). In addition, the histological examinations showed reduced distribution of Leydig cells per one  $\text{mm}^2$  of the interstitial tissue compared to control group ( $P > 0.05$ ). In line, the serum levels of testosterone (as biomarker for Leydig cells endocrine status) were analyzed. In contrast to those animals in 30 mg/kg NMCM-received group, the biochemical outcomes illustrated no significant changes for serum levels of testosterone in 7.5 mg/kg and 15 mg/kg NMCM-received groups compared to control group (Fig. 2).

#### 3.2. The NMCM decreased Bcl-2 expression and enhanced Bax expression

The expressions of Bcl-2 and Bax, as main regulators of mitochon-

dria-dependent apoptosis, were evaluated. The semi-quantitative RT-PCR results showed a remarkable ( $P < 0.05$ ) reduction in Bcl-2 mRNA levels in all three NMCM-received animals versus control group. No statistical differences were observed between NMCM-received groups. Similar to RT-PCR findings, the IHC analysis revealed a significant ( $P < 0.05$ ) decrement in percentage of Bcl-2-positive tubules in NMCM-received groups compared with control animals. To proof the last histologic data, the pixel-based histogram analysis was done. Observations showed intensive monotone Bcl-2-positive reactions per  $253 \times 10 \mu\text{m}$  of control group tubules. Meanwhile this ratio altered to low and focal positive reactions at same area in 15 mg/kg and 30 mg/kg NMCM-received groups (Fig. 3). In continue observations demonstrated a significant enhancement in Bax mRNA of NMCM-received animals (especially in those animals from 15 mg/kg and 30 mg/kg NMCM-received groups) versus control group. Moreover, the NMCM remarkably ( $P < 0.05$ ) enhanced the percentage of Bax-positive tubules in cross sections of 30 mg/kg NMCM-received animals compared with control, 7.5 mg/kg and 15 mg/kg NMCM-received groups. More analyses revealed a sharp Bax-positive reaction in pixel-based histogram analysis of cross sections from 30 mg/kg NMCM-received group (Fig. 4).

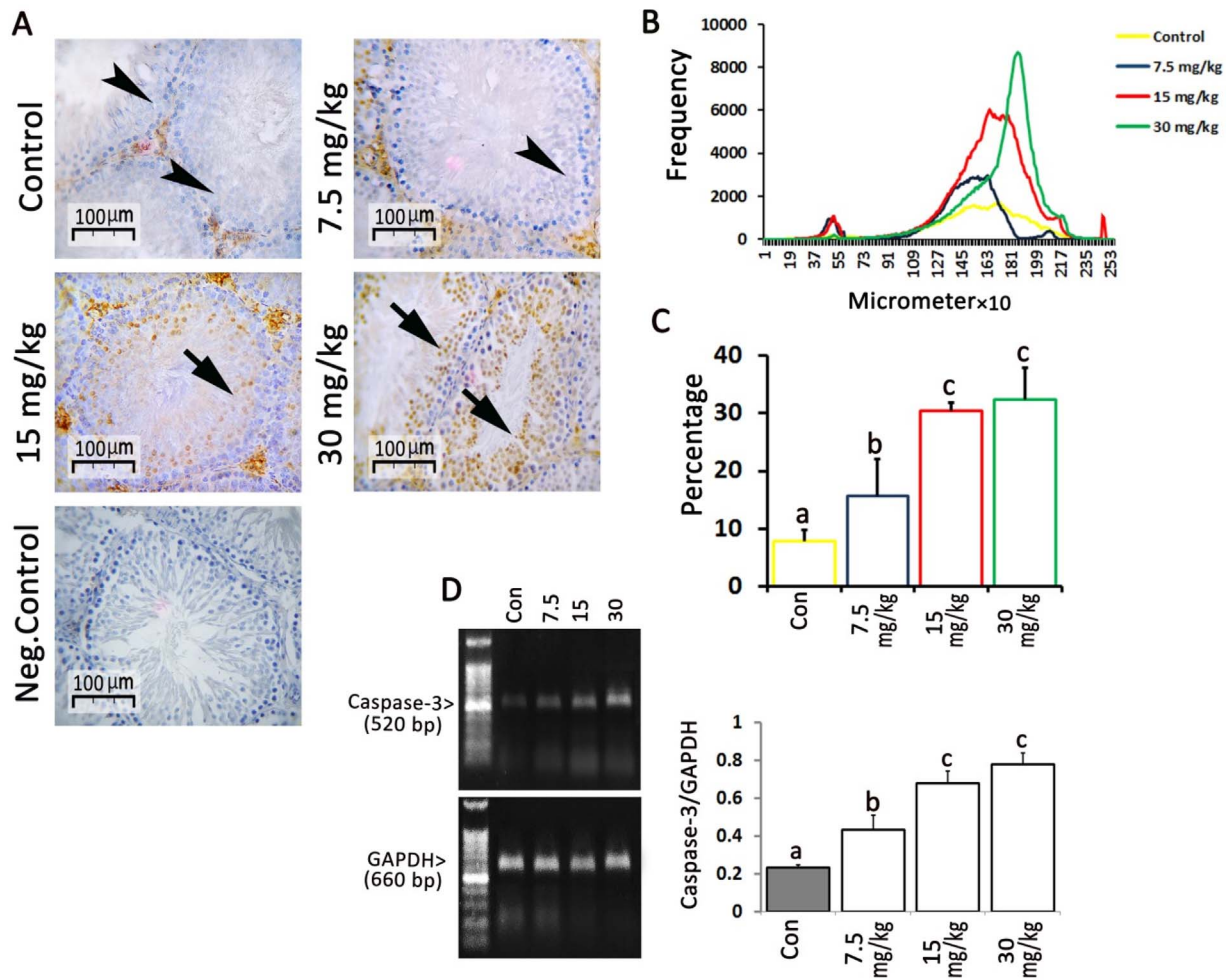


**Fig. 6.** (A) Immunohistochemical staining for caspase-3; see intact seminiferous tubules representing unstained cells (head arrows) and the tubule with impaired spermatogenesis presenting caspase-3-positive cells (arrows). **Neg. Control:** negative control, no primary antibody was used. (B) pixel based histogram analysis for caspase-3 positive reaction in  $253 \times 10 \mu\text{m}$  of one cross section, (C) percentage of seminiferous tubules with positive reaction for caspase-3 and (D) RT-PCR electrophoresis gel result. See relative semi-quantitative intensity (caspase-3/GAPDH) for increased caspase-3 mRNA level in NMCM-received groups versus control group. All data are presented in Mean  $\pm$  SD and <sup>a,b,c</sup> are representing significant differences ( $P < 0.05$ ) between marked groups.

### 3.3. The NMCM enhanced p53 and caspase-3 expression

The mRNA levels of p53 and caspase-3 were increased in NMCM-received groups ( $P < 0.05$ ) versus control group. Accordingly, the animals in 15 mg/kg and 30 mg/kg NMCM-received groups exhibited remarkably ( $P < 0.05$ ) higher p53 and caspase-3 mRNA levels compared to 7.5 mg/kg NMCM-received and control animals. A significant ( $P < 0.05$ ) elevation in percentage of p53 and caspase-3-positive tubules was revealed in NMCM-received groups. Moreover monotone and sharp enhancement of p53 and caspase-3-positive reactions was observed in pixel-based histogram analyses of cross sections from NMCM-received groups (Figs. 5 and 6).

### 3.4. The NMCM diminished PCNA expression

Observations revealed a remarkable ( $P < 0.05$ ) reduction in percentage of PCNA-positive tubules in the NMCM-received animals in comparison to control group. Additional pixel based histogram analysis showed the same result. Accordingly, the animals in NMCM-received group exhibited intensive monotone PCNA-positive reactions per  $253 \times 10 \mu\text{m}$  compared to low and focal reaction in cross sections from control group (Fig. 7).

### 3.5. The NMCM inflicted severe DNA fragmentation

DNA laddering test was done in order to analyze the DNA fragmentation as hallmark for apoptosis. Observations showed a severe DNA damage in 30 mg/kg NMCM-received animals. No DNA was observed in control group (Fig. 7D).

## 4. Discussion

Considering the important effect of novel social life and nutritional abuse on male reproductive status, recent concerns about the possible adverse effect of some supplementary chemicals/agents against fertilization potential have been increased. Indeed, given their antioxidant characteristics, the curcumin and albeite other antioxidants, including silymarin (Oufi et al., 2012), crocin (Bakhtiary et al., 2014), vitamin E (Chen et al., 2012) are widely used among population. However, some of these chemicals/agents are known for their adverse effect against spermatogenesis and/or follicular growth in both female and male humans and/or animal cases. Minding contrary reports about the adverse effect of curcumin on sperm quality (Mathuria and Verma, 2008; Naz, 2011) and considering its anti-proliferative characteristic (Lin et al., 2014), here in present study we aimed to investigate the effect of NMCM, as more effective small size agents, on spermatogenesis ratio as well as endocrine status in male rat models. Our findings

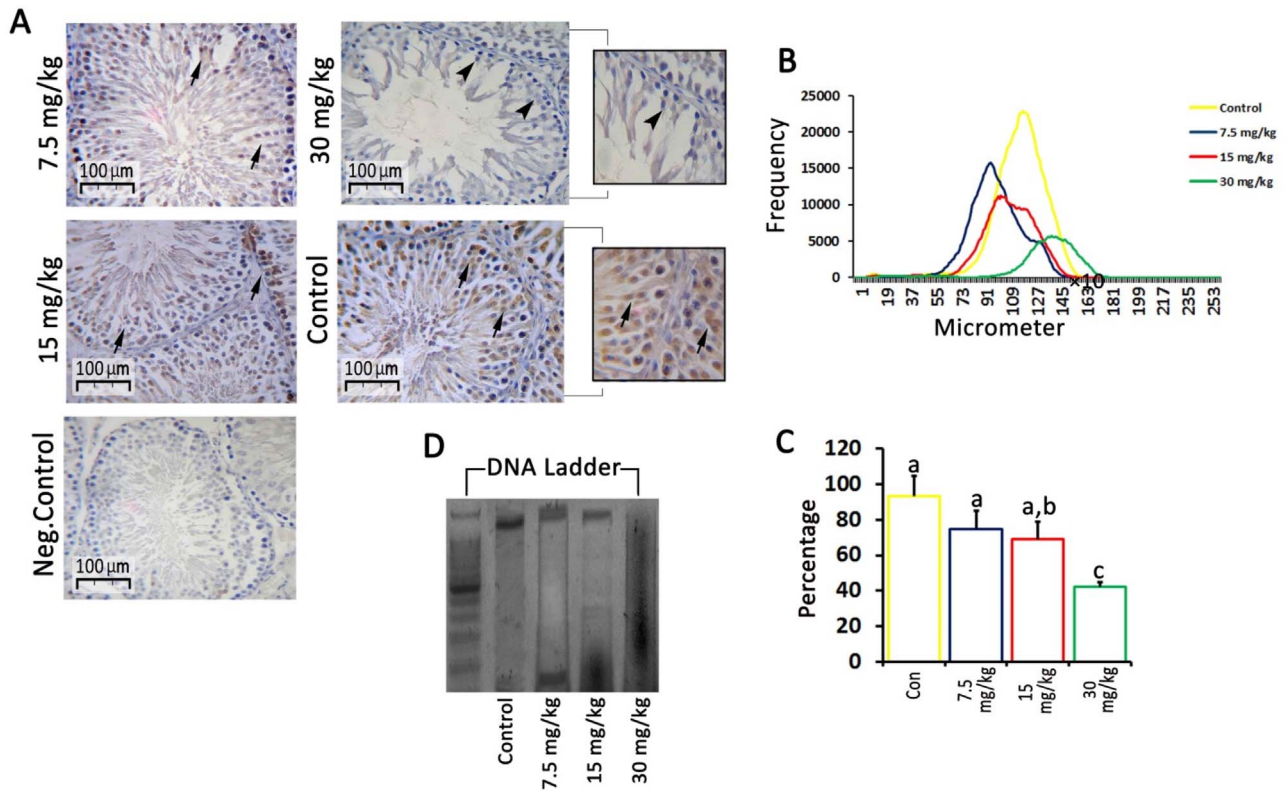


**Fig. 7.** (A) Immunohistochemical staining for PCNA; the cross section from control group represents high distribution of PCNA-positive cells (arrows), which is significantly decreased in cross section NMCM-received group (see head arrows for unstained cells). **Neg. Control:** negative control, no primary antibody was used, (B) pixel based histogram analysis for PCNA positive reaction in  $253 \times 10 \mu\text{m}$  of one cross section, (C) percentage of seminiferous tubules with positive reaction for PCNA and (D) DNA ladder test; See intact DNA in control group, the 7.5 mg/kg and 15 mg/kg NMCM-received groups are representing DNA fragmentation and the lane belonging to 30 mg/kg NMCM-received group is presenting severe DNA damage.

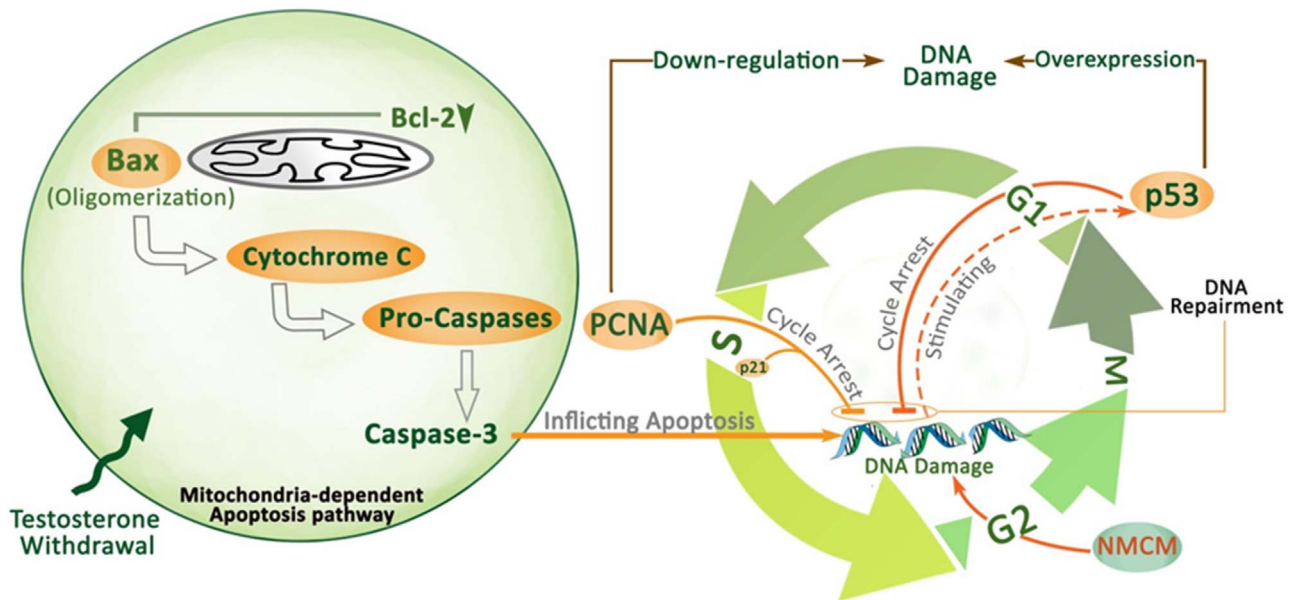


**Fig. 8.** Cross link between the NMCM-induced mitochondria-dependent apoptosis, p53 overexpression and DNA damage; suppressed testosterone secretion triggers the mitochondria-dependent apoptosis. Indeed, the NMCM by reducing the Bcl-2 and enhancing the Bax and caspase-3 expression, initiates the intrinsic apoptosis pathway. On the other hand, down-regulated PCNA expression (especially at dose level of 30 mg/kg), suppresses the PCNA/p21-related homeostasis reactions (DNA repairment) at S phase of cell cycle. The last event in association with highly expressed caspase-3 result in impressive DNA damage. Aside failed homeostasis, the inflicted DNA damage triggers the p53 over expression, which in turn promotes the apoptosis and DNA fragmentation. All these molecular alterations diminish cellularity, reduce tubular differentiation index and ultimately result in arrested spermatogenesis.

showed that, the NMCM, at administrated doses, elevated the histological damages, enhanced the Bax, p53, and caspase-3 expression, diminished Bcl-2 and PCNA expression, resulted in severe DNA fragmentation and reduced testicular endocrine status (Fig. 8).

Our preliminary histologic data exhibited spermatogenesis arrest, enhanced negative tubular differentiation index and reduced cellularity per tubule of cross sections from NMCM-received animals. On the other hand, a remarkable reduction in serum level of testosterone, as an

important marker for testicular endocrine function, was revealed in NMCM-received groups. Making a cross link between these two data, we can hypothesize that, reduced testosterone biosynthesis adversely affected the Sertoli cells supportive and physiologic interactions during spermatogenesis (Tesarik et al., 2002; Walker and Cheng, 2005), which in turn partially resulted in spermatogenesis arrest, diminished differentiation ratio and finally decreased cellularity.

Given that, the testosterone withdrawal triggers the apoptosis-related pathways (Sofikitis et al., 2008) and considering the pro-apoptotic characteristic of curcumin (Jiang et al., 2015), we focused on NMCM-induced impact against those genes involving in mitochondria-dependent apoptosis. In line, the Bcl-2 expression, as a member of anti-apoptotic proto-oncogenes, was examined. Indeed, the Bcl-2 preserves the mitochondrial membrane integrity during intrinsic apoptosis (Delbridge and Strasser, 2015). Thus, any reduction in Bcl-2 expression/stability leads to releasing of cytochrome c through mitochondrial membrane, which in turn results in caspases-dependent pathways (Chen et al., 2000; Chipuk and Green, 2008). Our RT-PCR as well as IHC analyses illustrated that the NMCM (especially at dose level of 30 mg/kg) significantly reduced the Bcl-2 expression. However to understand the delicate role of Bcl-2, one should note the fact that, the Bcl-2 and Bax are the hallmarks of intrinsic apoptosis and/or cell survival (Jiang et al., 2015). In fact the Bax, as a well-known pro-apoptotic protein, resides in cytosol and translocates to mitochondria upon apoptosis induction (Cassidy-Stone et al., 2008). In the case of stimulation (by activators and/or Bcl-2 suppression), the Bax proteins oligomerization enhances the mitochondrial membrane permeability. This last event, by disrupting the mitochondrial inner transmembrane potential triggers cytochrome C releasing and consequent caspase activation (Cassidy-Stone et al., 2008; Jiang et al., 2015; Karbowski et al., 2006). Minding increased Bax expression in NMCM-received groups, we can hypothesize that, the NMCM initiates the mitochondria-dependent apoptosis pathway not only by suppressing Bcl-2 expression but also by provoking the Bax over-expression in germ cell lineage. Thus it would be more logic to conclude that, similar to CMN-induced pro-apoptotic impact against carcinogenic cells, here in testicular tissue the NMCM is able to trigger the mitochondria-dependent intrinsic apoptosis pathway. Considering the nanomicelles safety, current characteristic basically may attribute to a cross link between the anti-proliferative nature of CMN and proliferative physiology of germ cells.

In continue, we assessed the caspase-3 expression as finisher of apoptosis story (Riedl and Shi, 2004). Observations showed a notable enhancement in caspase-3 expression in NMCM-received groups versus control animals. As a matter of fact, the caspase-3 activates cytoplasmic endonucleases. The endonucleases in turn degrade the nuclear materials, proteins and cytoskeletal architectures (McIlwain et al., 2013). Moreover, the caspase-3 cleaves the inhibitor of endonuclease caspase activated DNase (CAD), leading to chromosomal DNA fragmentation (Elmore, 2007). Thus, we assessed DNA fragmentation and observations demonstrated a severe DNA damage in testicles of 30 mg/kg NMCM-received group. The mystery is that, aside increased Bax, and caspase-3 and diminished Bcl-2 expression, why the animals in 7.5 mg/kg and 15 mg/kg NMCM-received groups exhibited intact DNA? In order to understand the subject one should note that, two p53 and PCNA proteins are known to progress hemostatic reactions related to DNA damage (Paunesku et al., 2001). In fact, the PCNA plays a crucial role in S phase of cell cycle by participating in DNA replication and DNA synthesis processes. During DNA replication, the PCNA first forms a complex with replication factor C (RFC a large nuclear complex). Consequently, the RFC-PCNA complex allows DNA polymerase  $\delta$  to bind PCNA and initiate DNA replication via binding to the RNA priming site (Strzalka and Ziemienowicz, 2011). Thus, any reduction in PCNA expression, results in DNA synthesis arrest and/or progressive DNA damage. (Cazzalini et al., 2010). On the other hand, the PCNA has been known as a dancer with different partners. For instance it has been illustrated that, the PCNA binds with GADD45 and p21 as p53-

inducible proteins and ultimately by this interaction regulates the DNA replication/repairment (De Oliveira et al., 2008; Pinheiro et al., 2007; Soria and Gottifredi, 2010). Actually, the tumor suppressor p53 protein is known as genome guardian, which breaks the cell cycle at G<sub>1</sub>/S and G<sub>2</sub>/M phases following DNA damage. Thus, the p53 permits the cell repairing DNA fragmentation (Barnum and O'Connell, 2014). Meanwhile, the P53 is able to initiate apoptosis as well. Accordingly, the p53 through directly/indirectly up-regulating the Bax and Bak expression (Hemann and Lowe 2006), via sensitizing cells to death receptor ligands (Petak et al., 2000) and triggering caspases activation (MacLachlan and El-Deiry., 2002) handles the apoptosis. Therefore, here in present study we analyzed the PCNA and p53 expression. Observations revealed mild p53 expression (mRNA) in 7.5 mg/kg, sharp enhancement in 15 mg/kg groups as well as notable reduction in 30 mg/kg NMCM-received animals. On the other hand, the animals in 7.5 mg/kg and 15 mg/kg NMCM-received groups exhibited significantly higher percentage of PCNA-positive tubules versus 30 mg/kg NMCM-received group. Reconsidering our findings we can suggest that, the p53 overexpression in 7.5 mg/kg and 15 mg/kg NMCM-received groups, provided appropriate enough period for PCNA involvement in DNA repairment/synthesis. Meanwhile, diminished p53 and PCNA expression (as preserving elements) fairly resulted in severe DNA fragmentation in 30 mg/kg NMCM-received animals.

## 5. Conclusion

Our data showed that, the NMCM by a- reducing the testicular endocrine status, b- down-regulating Bcl-2 expression and c- by enhancing the Bax and caspase-3 expression, initiates the intrinsic apoptosis pathway. On the other hand, it down-regulates the p53 and PCNA expression (at dose level of 30 mg/kg), which in turn suppresses the p53 and PCNA-related hemostasis reactions. All mentioned molecular alterations are responsible for significant reduction in cellularity and tubular differentiation index as well as spermatogenesis.

## Conflict of interest

Non declared.

## Acknowledgments

Authors would like to thank department of Biology, Faculty of Basic science and Urmia University for financial support. This manuscript is a part of thesis NO: 2-112, which is approved by scientific deputy of Urmia University.

## References

- Amaral, J.D., Xavier, J.M., Steer, C.J., Rodrigues, C.M., 2010. The role of p53 in apoptosis. *Discov. Med.* 9 (45), 145–152.
- Bakhtyari, Z., Shahrooz, R., Ahmadi, A., Zarei, L., 2014. Evaluation of antioxidant effects of crocin on sperm quality in cyclophosphamide treated adult mice. *Vet. Res. Forum* 5 (3), 213–218.
- Barnum, K.J., O'Connell, M.J., 2014. Cell cycle regulation by checkpoints. *Methods Mol. Biol.* 1170, 29–40.
- Cao, J., Jia, L., Zhou, H.M., Liu, Y., Zhong, L.F., 2006. Mitochondrial and nuclear DNA damage induced by curcumin in human hepatoma G2 cells. *Toxicol. Sci.* 91 (2), 476–483.
- Cassidy-Stone, A., Chipuk, J.E., Ingerman, E., Song, C., Yoo, C., Kuwana, T., Kurth, M.J., Shaw, J.T., Hinshaw, J.E., Green, D.R., Nunnari, J., 2008. Chemical inhibition of the mitochondrial division dynamin reveals its role in Bax/Bak-dependent mitochondrial outer membrane permeabilization. *Dev. Cell* 14 (2), 193–204.
- Cazzalini, O., Scovassi, A.I., Savio, M., Stivala, L.A., Prosperi, E., 2010. Multiple roles of the cell cycle inhibitor p21(CDKN1A) in the DNA damage response. *Mutat. Res.* 704 (1–3), 12–20.
- Chen, Q., Gong, B., Almasan, A., 2000. Distinct stages of cytochrome c release from mitochondria: evidence for a feedback amplification loop linking caspase activation to mitochondrial dysfunction in genotoxic stress induced apoptosis. *Cell Death Differ.* 7 (2), 227–233.
- Chen, H., Zhao, H.X., Huang, X.F., Chen, G.W., Yang, Z.X., Sun, W.J., Tao, M.H., Yuan, Y., Wu, J.Q., Sun, F., Dai, Q., Shi, H.J., 2012. Does high load of oxidants in human semen

- contribute to male factor infertility? *Antioxid. Redox Signal.* 16 (8), 754–759.
- Chipuk, J.E., Green, D.R., 2008. How do BCL-2 proteins induce mitochondrial outer membrane permeabilization? *Trends Cell Biol.* 18 (4), 157–164.
- Chomczynski, P., Sacchi, N., 2006. The single-step method of RNA isolation by acid guanidinium thiocyanate-phenol-chloroform extraction: twenty-something years on. *Nat. Protoc.* 1 (2), 581–585.
- Choudhary, N., Sekhon, B.S., 2012. Potential therapeutic effect of curcumin-an update. *Pharm. Educ. Res.* 3 (2), 64.
- De Oliveira, M.G., Lauxen Ida, S., Chaves, A.C., Rados, P.V., Sant'Ana Filho, M., 2008. Immunohistochemical analysis of the patterns of p53 and PCNA expression in odontogenic cystic lesions. *Med Oral Patol. Oral Cir. Bucal.* 13 (5), E275–280.
- Delbridge, A.R., Strasser, A., 2015. The BCL-2 protein family, BH3-mimetics and cancer therapy. *Cell Death Differ.* 22 (7), 1071–1080.
- Elmore, S., 2007. Apoptosis: a review of programmed cell death. *Toxicol. Pathol.* 35 (4), 495–516.
- Gundewar, C., Ansari, D., Tang, L., Wang, Y., Liang, G., Rosendahl, A.H., Saleem, M.A., Andersson, R., 2015. Antiproliferative effects of curcumin analog L49H37 in pancreatic stellate cells: a comparative study. *Ann. Gastroenterol.* 28 (3), 391–398.
- Hemann, M.T., Lowe, S.W., 2006. The p53-Bcl-2 connection. *Cell Death Differ.* 13 (8), 1256–1259.
- Hu, M., Du, Q., Vancurova, I., Lin, X., Miller, E.J., Simms, H.H., Wang, P., 2005. Proapoptotic effect of curcumin on human neutrophils: activation of the p38 mitogen-activated protein kinase pathway. *Crit. Care Med.* 33 (11), 2571–2578.
- Jiang, A.J., Jiang, G., Li, L.T., Zheng, J.N., 2015. Curcumin induces apoptosis through mitochondrial pathway and caspases activation in human melanoma cells. *Mol. Biol. Rep.* 42 (1), 267–275.
- Karbowski, M., Norris, K.L., Cleland, M.M., Jeong, S.Y., Youle, R.J., 2006. Role of Bax and Bak in mitochondrial morphogenesis. *Nature* 443 (7112), 658–662.
- Kermer, P., Klocker, N., Labes, M., Thomsen, S., Srinivasan, A., Bahr, M., 1999. Activation of caspase-3 in axotomized rat retinal ganglion cells in vivo. *FEBS Lett.* 453 (3), 361–364.
- Keshavarz, R., Bakhshinejad, B., Babashah, S., Baghi, N., Sadeghizadeh, M., 2016. Dendrosomal nanocurcumin and p53 overexpression synergistically trigger apoptosis in glioblastoma cells. *Iran. J. Basic Med. Sci.* 19 (12), 1353–1362.
- Kolasa, A., Misiakiewicz, K., Marchlewicz, M., Wiszniewska, B., 2012. The generation of spermatogonial stem cells and spermatogonia in mammals. *Reprod. Biol.* 12 (1), 5–23.
- Kumaravel, M., Sankar, P., Rukkumani, R., 2012. Antiproliferative effect of an analog of curcumin bis-1,7-(2-hydroxyphenyl)-hepta-1,6-diene-3,5-dione in human breast cancer cells. *Eur. Rev. Med. Pharmacol. Sci.* 16 (14), 1900–1907.
- Li, Q., Falsey, R.R., Gaitonde, S., Sotello, V., Kislin, K., Martinez, J.D., 2007. Genetic analysis of p53 nuclear importation. *Oncogene* 26 (57), 7885–7893.
- Li, W., Wang, Y., Song, Y., Xu, L., Zhao, J., Fang, B., 2015. A preliminary study of the effect of curcumin on the expression of p53 protein in a human multiple myeloma cell line. *Oncol. Lett.* 9 (4), 1719–1724.
- Lin, W.-Y., Cooper, C., Camarillo, I., Reece, L.M., Clah, L., Natarajan, A., Campana, L.G., Sundararajan, R., 2014. The effectiveness of electroporation-based nanocurcumin and curcumin treatments on human Breast cancer cells. *Proc. ESA Annual Meeting on Electrostatics 1*.
- Lu, W.J., Chapo, J., Roig, I., Abrams, J.M., 2010. Meiotic recombination provokes functional activation of the p53 regulatory network. *Science* 328 (5983), 1278–1281.
- Lukas, J., Lukas, C., Bartek, J., 2011. More than just a focus: the chromatin response to DNA damage and its role in genome integrity maintenance. *Nat. Cell Biol.* 13 (10), 1161–1169.
- MacLachlan, T.K., El-Deiry, W.S., 2002. Apoptotic threshold is lowered by p53 transactivation of caspase-6. *Proc. Natl. Acad. Sci. U. S. A.* 99 (14), 9492–9497.
- Malani, N., Ichikawa, H., 2007. Curcumin: the Indian spice. *Adv. Exp.* 8.
- Mathuria, N., Verma, R.J., 2008. Curcumin ameliorates aflatoxin-induced toxicity in mice spermatozoa. *Fertil. Steril.* 90 (3), 775–780.
- McIlwain, D.R., Berger, T., Mak, T.W., 2013. Caspase functions in cell death and disease. *Cold Spring Harb. Perspect. Biol.* 5 (4), a008656.
- Mehta, K., Pantazis, P., McQueen, T., Aggarwal, B.B., 1997. Antiproliferative effect of curcumin (diferuloylmethane) against human breast tumor cell lines. *Anticancer Drugs* 8 (5), 470–481.
- Meistrich, M.L., 2013. Effects of chemotherapy and radiotherapy on spermatogenesis in humans. *Fertil. Steril.* 100 (5), 1180–1186.
- Naz, R.K., 2011. Can curcumin provide an ideal contraceptive? *Mol. Reprod. Dev.* 78 (2), 116–123.
- Nowshen, S., Yang, E.S., 2012. The intersection between DNA damage response and cell death pathways. *Exp. Oncol.* 34 (3), 243–254.
- Ortega, S., Prieto, I., Odajima, J., Martin, A., Dubus, P., Sotillo, R., Barbero, J.L., Malumbres, M., Barbacid, M., 2003. Cyclin-dependent kinase 2 is essential for meiosis but not for mitotic cell division in mice. *Nat. Genet.* 35 (1), 25–31.
- Oufi, H.G., Al-Shawi, N.N., Hussain, S.A., 2012. What are the effects of silibinin on testicular tissue of mice? *J. Appl. Pharm. Sci.* 2 (11), 9.
- Paunescu, T., Mittal, S., Protic, M., Oryhon, J., Korolev, S.V., Joachimiak, A., Woloschak, G.E., 2001. Proliferating cell nuclear antigen (PCNA): ringmaster of the genome. *Int. J. Radiat. Biol.* 77 (10), 1007–1021.
- Petak, I., Tillman, D.M., Houghton, J.A., 2000. p53 dependence of Fas induction and acute apoptosis in response to 5-fluorouracil-leucovorin in human colon carcinoma cell lines. *Clin. Cancer Res.* 6 (11), 4432–4441.
- Pinheiro, G.S., Silva, M.R., Rodrigues, C.A., Kerbaury, J., de Oliveira, J.S., 2007. Proliferating cell nuclear antigen (PCNA), p53 and MDM2 expression in Hodgkins disease. *Sao Paulo Med. J.* 125 (2), 77–84.
- Ragheb, A.M., Sabaneh Jr., E.S., 2010. Male fertility-implications of anticancer treatment and strategies to mitigate gonadotoxicity. *Anticancer Agents Med. Chem.* 10 (1), 92–102.
- Riedl, S.J., Shi, Y., 2004. Molecular mechanisms of caspase regulation during apoptosis. *Nat. Rev. Mol. Cell Biol.* 5 (11), 897–907.
- Rogério, F., Jordao Jr., H., Vieira, A.S., Maria, C.C., Santos de Rezende, A.C., Pereira, G.A., Langone, F., 2006. Bax and Bcl-2 expression and TUNEL labeling in lumbar enlargement of neonatal rats after sciatic axotomy and melatonin treatment. *Brain Res.* 1112 (1), 80–90.
- Rotgers, E., Nurmio, M., Pietila, E., Cisneros-Montalvo, S., Toppari, J., 2015. E2F1 controls germ cell apoptosis during the first wave of spermatogenesis. *Andrology* 3 (5), 1000–1014.
- Shaha, K., Tripathi, R., Mishra, D.P., 2010. Male germ cell apoptosis: regulation and biology. *Philos. Trans. R. Soc. Lond. B Biol. Sci.* 365 (1546), 1501–1515.
- Sofikitis, N., Giotitis, N., Tsounapi, P., Baltogiannis, D., Giannakis, D., Pardalidis, N., 2008. Hormonal regulation of spermatogenesis and spermiogenesis. *J. Steroid Biochem. Mol. Biol.* 109 (3), 323–330.
- Soleimani Asl, S., Farhadi, M.H., Moosavizadeh, K., Samadi Kuchak Sarai, A., Soleimani, M., Jamei, S.B., Joghataei, M.T., Samzadeh-Kermani, A., Hashemi-Nasl, H., Mehdizadeh, M., 2012. Evaluation of Bcl-2 family gene expression in hippocampus of 3, 4-methylenedioxymethamphetamine treated rats. *Cell J.* 13 (4), 275–280.
- Soria, G., Gottifredi, V., 2010. PCNA-coupled p21 degradation after DNA damage: the exception that confirms the rule? *DNA Repair (Amst.)* 9 (4), 358–364.
- Stoimenov, I., Helleday, T., 2009. PCNA on the crossroad of cancer. *Biochem. Soc. Trans.* 37 (Pt 3), 605–613.
- Strzalka, W., Ziemienowicz, A., 2011. Proliferating cell nuclear antigen (PCNA): a key factor in DNA replication and cell cycle regulation. *Ann. Bot.* 107 (7), 1127–1140.
- Tasdemir, E., Maiuri, M.C., Galluzzi, L., Vitale, I., Djavaheri-Mergny, M., D'Amelio, M., Criollo, A., Morselli, E., Zhu, C., Harper, F., 2008. Regulation of autophagy by cytoplasmic p53. *Nat. Cell Biol.* 10 (6), 676–687.
- Tesarik, J., Martinez, F., Rienzi, L., Iacobelli, M., Ubaldi, F., Mendoza, C., Greco, E., 2002. In-vitro effects of FSH and testosterone withdrawal on caspase activation and DNA fragmentation in different cell types of human seminiferous epithelium. *Hum. Reprod.* 17 (7), 1811–1819.
- Trivedi, R., Kompella, U.B., 2010. Nanomicellar formulations for sustained drug delivery: strategies and underlying principles. *Nanomedicine (Lond.)* 5 (3), 485–505.
- Uygur, R., Aktas, C., Tulubas, F., Uygur, E., Kanter, M., Erboglu, M., Caglar, V., Topcu, B., Ozen, O.A., 2014. Protective effects of fish omega-3 fatty acids on doxorubicin-induced testicular apoptosis and oxidative damage in rats. *Andrologia* 46 (8), 917–926.
- Vadlapudi, A.D., Mitra, A.K., 2013. Nanomicelles: an emerging platform for drug delivery to the eye. *Ther. Deliv.* 4 (1), 1–3.
- Walker, W.H., Cheng, J., 2005. FSH and testosterone signaling in Sertoli cells. *Reproduction* 130 (1), 15–28.
- Western, P.S., Miles, D.C., van den Bergen, J.A., Burton, M., Sinclair, A.H., 2008. Dynamic regulation of mitotic arrest in fetal male germ cells. *Stem Cells* 26 (2), 339–347.
- Xu, B., Hua, J., Zhang, Y., Jiang, X., Zhang, H., Ma, T., Zheng, W., Sun, R., Shen, W., Sha, J., Cooke, H.J., Shi, Q., 2011. Proliferating cell nuclear antigen (PCNA) regulates primordial follicle assembly by promoting apoptosis of oocytes in fetal and neonatal mouse ovaries. *PLoS One* 6 (1), e16046.
- Yang, C.W., Chang, C.L., Lee, H.C., Chi, C.W., Pan, J.P., Yang, W.C., 2012. Curcumin induces the apoptosis of human monocytic leukemia THP-1 cells via the activation of JNK/ERK pathways. *BMC Compl. Altern. Med.* 12, 22.
- Ye, M., Zhang, J., Zhang, J., Miao, Q., Yao, L., Zhang, J., 2015. Curcumin promotes apoptosis by activating the p53-miR-192-5p/215-XIAP pathway in non-small cell lung cancer. *Cancer Lett.* 357 (1), 196–205.
- Yokoyama, M., 2014. Polymeric micelles as drug carriers: their lights and shadows. *J. Drug Target.* 22 (7), 576–583.
- Zhou, Q.M., Wang, X.F., Liu, X.J., Zhang, H., Lu, Y.Y., Su, S.B., 2011. Curcumin enhanced antiproliferative effect of mitomycin C in human breast cancer MCF-7 cells in vitro and in vivo. *Acta Pharmacol. Sin.* 32 (11), 1402–1410.